Journal of Dentistry 61 (2017) 12–20

Contents lists available at ScienceDirect

Journal of Dentistry

journal homepage: www.elsevier.com/locate/jdent

The role of copper nanoparticles in an etch-and-rinse adhesive on antimicrobial activity, mechanical properties and the durability of resin-dentine interfaces

Mario F. Gutiérrez[a,b], Pamela Malaquias[a], Viviane Hass[c,d], Thalita P. Matos[a], Lucas Lourenço[a], Alessandra Reis[e], Alessandro D. Loguercio[e,*], Paulo Vitor Farago[f]

[a] School of Dentistry, State University of Ponta Grossa, Ponta Grossa, PR, Brazil
[b] Institute for Research of Dental Sciences, Faculty of Dentistry, University of Chile, Santiago, Chile
[c] Undergraduate and Post-Graduate Department, University CEUMA, São Luís, MA, Brazil
[d] Post-Graduate Department, State University of West Paraná, Cascavel, PR, Brazil
[e] Department of Restorative Dentistry, State University of Ponta Grossa, Ponta Grossa, PR, Brazil
[f] Department of Pharmaceutical Sciences, State University of Ponta Grossa, Ponta Grossa, PR, Brazil

ARTICLE INFO

Keywords:
Adhesive system
Copper nanoparticles
Antimicrobial activity
Knoop microhardness
Degree of conversion
Resin-dentine bond strength
Nanoleakage

ABSTRACT

Objectives: To evaluate the effect of addition of copper nanoparticles at different concentrations into an etch-and-rinse adhesive (ER) on antimicrobial activity, Knoop microhardness (KHN), *in vitro* and *in situ* degree of conversion (DC), as well as the immediate (IM) and 2-year (2Y) resin-dentine bond strength (μTBS) and nanoleakage (NL).

Methods: Seven experimental ER adhesives were formulated according to the amount of copper nanoparticles incorporated into the adhesives (0 [control], 0.0075 to 1 wt.%). We tested the antimicrobial activity of adhesives against *Streptococcus mutans* using agar diffusion assay after IM and 2Y. The Knoop microhardness and *in vitro* DC were tested after IM and 2Y. The adhesives were applied to flat occlusal dentine surfaces after acid etching. After resin build-ups, specimens were longitudinally sectioned to obtain beam-like resin-dentine specimens (0.8 mm^2), which were used for evaluation of μTBS and nanoleakage at the IM and 2Y periods. In situ DC was evaluated at the IM period in these beam-like specimens. Data were submitted to appropriate statistical analyses ($\alpha = 0.05$).

Results: The addition of copper nanoparticles provided antimicrobial activity to the adhesives only in the IM evaluation and slightly reduced the KHN, the *in vitro* and *in situ* DC (copper concentrations of 1 wt.%). However, KHN increase for all concentrations after 2Y. After 2Y, no significant reductions of μTBS (0.06 to 1% wt.%) and increases of nanoleakage were observed for copper containing adhesives compared to the control group.

Conclusion: Copper nanoparticles addition up to 0.5 wt.% may provide antimicrobial properties to ER adhesives and prevent the degradation of the adhesive interface, without reducing the mechanical properties of the formulations.

1. Introduction

Failure of composite restorations by secondary caries is considered the major reason for restoration replacement, which results in millions of dental care dollars spent annually [1–7]. The higher accumulation of dental biofilm around composite resin restorations than other materials or intact enamel are likely responsible for the faster degradation of these restorations [8–13]. Furthermore, composite resin undergoes volumetric contraction during polymerization, which have a great impact on their sealing ability. This can result in the formation of gaps between the adhesive resin and the dental structure [14].

In the oral environment, water, enzymes, occlusal stresses (generated during mastication and especially during parafunctional activities), temperature and microorganisms derived from plaque biofilms challenge the resin-dentine interface [14–16]. *S. mutans* and other bacterial species can then bond to this suitable biofilm and, in the presence of gaps and weakened interface, may invade the inner area of teeth and allow for the development of caries adjacent to tooth-restorative margins [16,17]. There seems to be an association between failure of the resin-dentine interface and increased levels of cariogenic

* Corresponding author at: Universidade Estadual de Ponta Grossa, Departamento de Odontologia, Avenida Carlos Cavalcanti, 4748 – Uvaranas, Ponta Grossa, Paraná, CEP: 84030-900, Brazil.
E-mail addresses: aloguercio@hotmail.com, alelog@uepg.br (A.D. Loguercio).

http://dx.doi.org/10.1016/j.jdent.2017.04.007
Received 30 October 2016; Received in revised form 14 April 2017; Accepted 18 April 2017

bacteria at the perimeter of resin composite restorations [14,16]. Production of acids [18] and esterases [19] may also accelerate the degradation of the hybrid layer, being an important factor in the premature failure of moderate-to-large composite restorations [14,16].

Although biofilm cannot be eliminated [20], one can reduce the pathogenicity of biofilm and make the restorative interface less prone to caries adjacent to restorations [16,17]. This can be achieved by developing dental materials with antibacterial properties to reduce biofilm formation at the tooth-restoration margins, without compromise the mechanical properties of the adhesive formation [21–23].

Among the most promising agents with antibacterial properties are metallic nanoparticles, which exhibit increased chemical activity and biocide effectiveness [24]. The antibacterial activity of copper [25–27] and silver nanoparticles [28,29] has been extensively investigated. Copper nanoparticles showed higher antibacterial activity compared with silver nanoparticles against *Escherichia coli, Bacillus subtilis and Staphylococcus aureus* [30,31]. In addition to superior antimicrobial activity, copper is cheaper than silver, easily available and the synthesis of copper nanoparticles is cost effective [32]. An additional advantage of copper nanoparticles is that they are easily oxidizable in air or aqueous media producing copper oxide nanoparticles. Copper oxide has an effective bactericidal action and can be easily blended with polymers or macromolecules producing stable polymers in regards to chemical and physical properties [33–36].

In dentistry, silver nanoparticles incorporation in resin cement and dental adhesives showed high antimicrobial activity and also improved mechanical and adhesive properties [37,38]. Incorporation of copper was also evaluated in several dental materials, such as glass ionomer [39], dental adhesive [40,41] and even dental implant [42,43]. In dental adhesives, only two recent studies used copper nanoparticles to test the effectiveness of these materials against *S. mutans* [40,41], However, none of these studies evaluated the mechanical properties of the adhesive, and hence the effect of different copper concentrations on them. In terms of bond strength, only Sabatini et al. [40] evaluated the immediate strength of the adhesive interface, and no study so far addressed the effects of copper addition on the long-term resin-dentine interface. Additionally, the literature still lacks information about the optimal copper concentration that can be added to an adhesive system to express its antimicrobial activity without jeopardizing other mechanical properties.

Therefore, we designed this *in vitro* study to investigate the effect of addition of copper nanoparticles at different concentrations into a simplified etch-and-rinse adhesive system on the antimicrobial activity, Knoop microhardness, *in vitro* and *in situ* degree of conversion, as well as the immediate and 2-year resin-dentine bond strength and nanoleakage.

2. Materials and methods

2.1. Formulation of the experimental adhesives and characterization of the copper nano-powder by FE-SEM and EDX

We formulated experimental adhesives using the simplified etch-and-rinse adhesive system (Ambar [AM], FGM Prod. Odont. Ltda, Joinville, SC, Brazil). All adhesives were formulated by adding different concentrations of copper nanoparticles (99.9% pure, SkySpring Nanomaterials, Inc., Houston, TX, USA; www.ssnano.com) (wt%): 0% (control, commercial material), 0.0075%, 0.015%, 0.06%, 0.1%, 0.5% and 1.0%.

The copper nanoparticles used for production of the experimental adhesives were characterized by field emission scanning electron microscope (FE-SEM) and energy dispersive X-ray (EDX) analysis. The incorporation to the adhesive solution was done in a dark room with a motorized stirrer.

2.2. Antimicrobial activity

After isolating a metallic matrix (5.8 mm diameter, 1.0 mm thick) with a very thin layer of petroleum jelly, we dispensed the adhesive until completely fill the mold. All visible air bubbles trapped in the adhesives specimens were carefully removed with a microbrush (Microbrush International, Grafton, WI, USA). An air stream was applied for solvent evaporation for 40 s at a distance of 10 cm.

Under a plastic matrix strip, the adhesive specimens were light-cured for 40 s with a LED light source at 1200 mW/cm^2 (Radii-cal, SDI, Baywater, Victoria, Australia), in close contact with each disc-like specimen. After polymerization, the specimens were removed from the mold, and polished with 600-grit SiC paper in order to remove the adhesive excesses and the oxygen-inhibition layer. Five adhesive discs of each group were made.

All specimens were stored in a dark vial for 24 h and each side of the specimen was disinfected by ultraviolet light with a 30 min exposure. They were placed on brain heart infusion (BHI) agar plates (Kasvi Ltda, Curitiba, PR, Brasil) containing a freshly prepared lawn of *S. mutans* (ATCC 25175). *S. mutans* was cultured microaerophilically in brain heart infusion broth (Difco Laboratories, Detroit, MI, USA) for 72 h at 37 °C. Then, 100 µL of the bacterial suspension was swabbed onto BHI to create the lawn [44,45] and the BHI agar plates were stored in an anaerobic jar. The inhibition zones (mm) were measured after 96 h with a digital caliper to the nearest 0.1 mm (Absolute Digimatic, Mitutoyo, Tokyo, Japan).

2.3. Knoop microhardness

Five adhesive discs of each group were produced as described for microbiological test. After preparation, specimens were stored in a dark vial for 24 h or after 2 year of water storage before microhardness measurement. Specimens were then taken to a HMV-2 microhardness tester (Shimadzu; Tokyo, Japan) equipped with a Knoop indenter. Five measurements were performed of each specimen with a load of 10 g for 15 s. The first measurement was performed in the center of the adhesive disc. The other four measurements were performed 100 µm and 200 µm to the left and right of the first one. Values obtained for the same specimen were averaged for statistical purposes [46].

2.4. In vitro degree of conversion

Ten new adhesive discs of each group were produced as described for microbiological tests. Specimens were stored in wet environment for 24 h at 37 °C prior to performing the DC readings. The DC measurements were performed in a micro-Raman spectrometer (Bruker Optik GmbH, Ettlingen, Baden-Württemberg, Germany).

The micro-Raman spectrometer was first calibrated for zero and then for coefficient values using a silicon specimen. Specimens were analyzed using the following micro-Raman parameters: 20-mW Neon laser with 532-nm wavelength, spatial resolution of ≈3 µm, spectral resolution ≈5 cm^{-1}, accumulation time of 20 s with 6 co-additions, and magnification of 20X (Olympus UK, London, UK) to beam diameter of ≈1 µm [47,48]. The spectra were taken at three different sites for each specimen and the values averaged for statistical purposes. Spectra of uncured adhesives were taken as reference. Post-processing of spectra was performed using the dedicated Opus Spectroscopy Software version 6.5 (Bruker Optik GmbH, Ettlingen, Baden- Württemberg, Germany).

The ratio of double-bond content of monomer to polymer in the adhesive was calculated according to the following formula: DC (%) = $(1–R_{cured}/R_{uncured}) \times 100$, where R is the ratio of aliphatic and aromatic peak areas at 1639 cm^{-1} and 1609 cm^{-1} in cured and uncured adhesives.

2.5. Teeth preparation and bonding procedures

The University Ethics Committee approved this part of the experiment under protocol number 1.065.446. Thirty-five caries-free extracted human third molars, collected from patients with age ranging from 18 to 35 years old, were randomly distributed among 7 groups by lottery. The teeth were collected after the patient's informed consent. Teeth were disinfected in 0.5% chloramine, stored in distilled water and used within 3 months after extraction. A flat dentine surface was exposed on each tooth after wet grinding the occlusal enamel with 180-grit SiC paper. The enamel-free, exposed dentine surfaces were further polished with 600-grit silicon-carbide paper for 60 s to standardize the smear layer.

The adhesives were applied as per manufacturers' instructions. The dentine surfaces were acid etched with 37% phosphoric acid for 15 s, water rinsed for 15 s and dried with absorbent paper keeping the dentine surface slightly wet. Two adhesive coats were vigorously applied by rubbing the adhesive for 20 s (10 s each coat). Then, gently air stream of 10 s was applied for solvent evaporation and the adhesive layer was light cured with a LED light curing unit for 10 s at 1200 W/cm^2 (Radii-cal, SDI, Bayswater, Victoria, Australia). Resin composite blocks (Opallis, FGM) were buildup on the bonded surfaces in 3 increments of 1.0 mm thick each and each one was individually light activated for 40 s. A single operator carried out all bonding procedures in an environment with controlled temperature and humidity. Five teeth were used for each experimental group.

After storage of the bonded teeth in distilled water at 37 °C for 24 h, they were longitudinally sectioned in both "x" and "y" directions across the bonded interface with a diamond saw in a cutting machine (IsoMet 1000; Buehler, Lake Bluff, USA), under water cooling at 300 rpm to obtain resin-dentine beam-like specimens with a cross-sectional area of approximately 0.8 mm^2.

The number of premature failures (PF) per tooth during specimen preparation was recorded. The cross-sectional area of each beam-like specimen was measured with the digital caliper to the nearest 0.01 mm and recorded for subsequent calculation of the microtensile bond strength (μTBS) values (Absolute Digimatic, Mitutoyo, Tokyo, Japan). The resin-dentine beam-like specimens originated from the same tooth were randomly divided and assigned to be tested immediately or after 2-year of storage in distilled water at 37 °C. The storage solution was not changed and its pH was monitored monthly. The resin-dentine beam-like specimens from each tooth were then divided as follow:

- Two beam-like specimens at each storage period were used for nanoleakage evaluation.
- Two beam-like specimens were used to measure the immediate *in situ* degree of conversion.
- Two beam-like specimens at each storage period were used for identification of the presence of copper in the hybrid layer.
- The remaining beam-like specimens were submitted to μTBS test at each storage period.

2.6. Microtensile bond strength testing

Each beam-like specimens was attached to a modified device for microtensile bond strength test with cyanoacrylate resin (Super Bonder, Loctite, São Paulo, SP, Brazil) and subjected to a tensile force in a universal testing machine (Kratos, São Paulo, SP, Brazil) at 0.5 mm/min. The failure mode was evaluated at 40x (HMV-2, Shimadzu, Tokyo, Japan) and classified as cohesive in dentine (failure exclusive within cohesive dentine − CD); cohesive in resin (failure exclusive within cohesive resin − CR); adhesive (failure at resin/dentine interface − A), or mixed (failure at resin/dentine interface that included cohesive failure of the neighboring substrates, M). The number of premature failures (PF) was recorded and it was not included in the average mean bond strength.

2.7. Nanoleakage evaluation

All resin-dentine beam-like specimens selected for this test were coated with two layers of nail varnish applied up to within 1 mm of the bonded interfaces. The resin-dentine beam-like specimens were immersed in 50 wt% ammoniacal silver nitrate solution in total darkness for 24 h, rinsed thoroughly in distilled water, and immersed in photo developing solution for 8 h under a fluorescent light to reduce silver ions into metallic silver grains within voids along the bonded interface.

Specimens were mounted on aluminium stubs, polished with 1000-, 1500-, 2000- and 2500-grit SiC paper and 1 and 0.25 μm diamond paste (Buehler Ltd., Lake Bluff, IL, USA). Then, they were ultrasonically cleaned, air dried and gold sputter coated (MED 010, Balzers Union, Balzers, Liechtenstein). The interfaces were observed in a scanning electron microscope in the backscattered mode at 15 kV (VEGA 3 TESCAN, Shimadzu, Tokyo, Japan).

In a way to standardize image acquisition, three pictures were taken of each beam-like specimen. The first picture was taken in the center of the resin-dentine beam-like specimens. The other two pictures were taken 0.3 mm to the left and right of the first one. As two resin-dentine beam-like specimens per tooth were evaluated and a total of five teeth were used for each experimental condition, a total of 30 images were evaluated per group [49]. A technician who was blinded to the experimental conditions under evaluation took them all. The relative percentage of nanoleakage within the adhesive and hybrid layer areas was measured in all pictures using the public domain Image J software, a Java-based image processing software package developed at the National Institutes of Health (NIH) [50].

Before performing the nanoleakage test a pilot test was conducted to evaluate if the presence of copper in the adhesive could impair the visualization of silver nitrate uptake. For this purpose, we performed scanning electron microscopy (SEM) images of resin-dentine interfaces of all groups without immersion in silver nitrate. Even in adhesive interfaces with the highest copper concentration (1%), copper nanoparticles were not observed using the same parameters described above. And thus, the results of nanoleakage test reflect the amount of silver uptake into unpolymerized areas and/or nanospaces not infiltrated by the resin adhesive but not the presence of copper in the hybrid layer.

2.8. In situ degree of conversion within adhesive/hybrid layers

All resin-dentine beams selected for this test were wet polished using 1500; 2000; 2500 and 4000-grit SiC paper for 30 s each. The specimens were ultrasonically cleaned for 10 min and positioned into micro-Raman equipment. The DC measurements were performed in a micro-Raman spectrometer (Bruker Optik GmbH, Ettlingen, Baden-Württemberg, Germany). The micro-Raman spectrometer was first calibrated for zero and then for coefficient values using a silicon specimen. Specimens were analyzed using the following micro-Raman parameters: 20-mW Neon laser with 532-nm wavelength, spatial resolution of ≈3 μm, spectral resolution ≈5 cm^{-1}, accumulation time of 30 s with 6 co-additions, and magnification of 100X (Olympus UK, London, UK) to beam diameter of ≈1 μm [47,48,51]. The spectra were taken at the resin-dentine interface, in the middle of the hybrid layer within the intertubular dentine, at three different sites for each specimen and the values averaged for statistical purposes. Spectra of uncured adhesives were taken as reference. Post-processing of spectra was performed using the dedicated Opus Spectroscopy Software version 6.5 (Bruker Optik GmbH, Ettlingen, Baden-Württemberg, Germany). The ratio of double-bond content of monomer to polymer in the adhesive was calculated according to the formula described earlier in the materials and methods section in the item *in vitro* degree of conversion.

2.9. Identification of copper within adhesive itself and in the adhesive/hybrid layers by EDX

For the first analysis, three adhesive discs of each group were produced as described for the microbiological test. After preparation, specimens were stored in a dark vial for 24 h and vertically sectioned in the middle with a diamond saw in a cutting machine (IsoMet 1000; Buehler, Lake Bluff, USA), under water cooling (at 300 rpm). Then, 05 areas of this cross-sectional interface were evaluated under EDX.

In the second part, two beam-like specimens at each storage period previously obtained during specimens sectioning (item 2.5) were used for identification of the presence of copper in the hybrid layer. The analysis of the copper content in each selected beam was performed by field emission scanning electron microscope (FE-SEM) (MIRA 3 TESCAN, Shimadzu, Tokyo, Japan) coupled with an energy-dispersive X-ray spectrometer (EDX). The bonding area was observed and the analysis was focused to the middle of the hybrid layer. One site, randomly determined, per beam-like specimens was examined.

2.10. Statistical analysis

Data for microbiological test (mm), *in vitro degree of conversion* and *in situ* degree of conversion (%) were subjected to a one-way ANOVA. Data for microhardness (KNH) was subjected to a two-way ANOVA. For μTBS and nanoleakage, the experimental unit was the tooth with half being tested immediately and the other half after 2 years of water storage. The μTBS and nanoleakage values of all beam-like specimens from the same hemi-tooth were averaged for statistical purposes. The μTBS (MPa) and nanoleakage (%) data of each adhesive were subjected to two-way repeated measures ANOVA. The repeated measure was the tooth at the two-evaluation period. Tukey's post hoc test was used for pair-wise comparisons ($\alpha = 0.05$) using the Statistica for Windows software (StatSoft, Tulsa, OK, USA).

3. Results

The FE-SEM (Fig. 1) revealed that the copper particles have a nanometer size, ranging from 63 to 154 nm. As demonstrated in the EDX spectrum of a representative specimen (Fig. 2), the sample has a high percentage of copper atoms, without contamination by other elements.

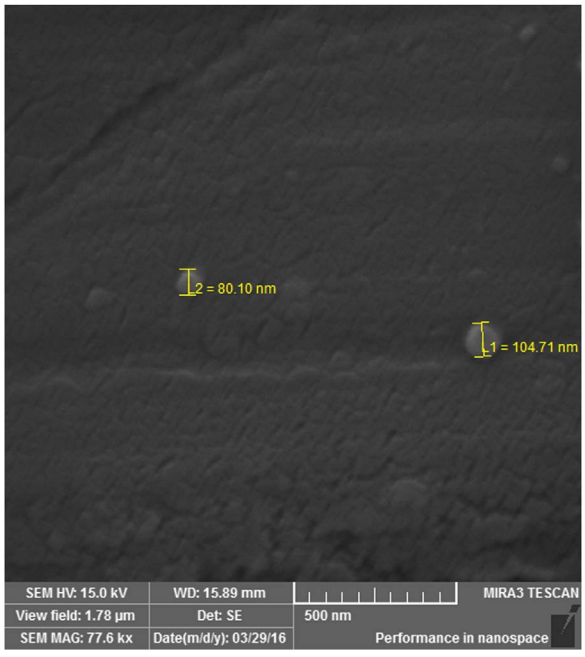

Fig. 1. Field emission scanning electron microscopy (FE-SEM) of the copper nanoparticles, demonstrating nanometer size.

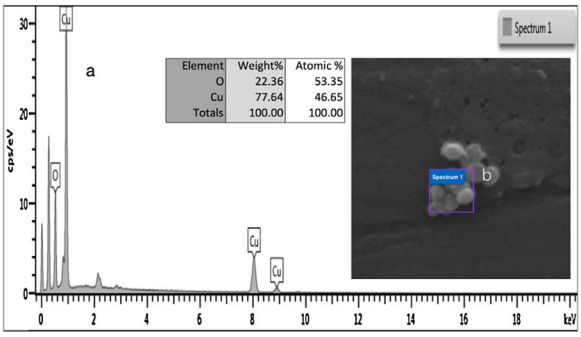

Fig. 2. EDX spectrum (a) from selected area of the copper nanoparticles powder sample outlined by a magenta rectangle in (b). The figure table summarizes the elemental composition of the sample area outlined.

3.1. Antimicrobial activity

Unfortunately, the 2-year specimens did not present any antibacterial response (data not shown). Thus, only the results from the immediate period will be described. Significant differences among groups were detected (Table 1; $p = 0.001$). All experimental copper-containing adhesives showed higher antibacterial properties against *Streptococcus mutans* than the control adhesive. The highest antimicrobial effect was observed in adhesives with the highest copper concentration (0.1, 0.5 and 1%).

3.2. Knoop microhardness, in vitro and in situ degree of conversion

The cross-product interaction of the two-way repeated measures ANOVA was statistically significant for microhardness (Table 2; $p = 0.0001$). Adhesive formulations with copper concentrations equal to or higher than 0.06% showed higher microhardness values than control and low-filled copper adhesives (Table 2). After 2 years of water storage, the control group showed the same microhardness, however, all copper containing-adhesives showed significant improvement of the microhardness (Table 2).

For *in vitro* and *in situ* DC, one-way ANOVA showed significant differences among experimental groups (Table 2; $p < 0.03$). Only the adhesive with 1 wt% copper concentration was significant different than the other formulations ($p = 0.02$ and $p = 0.03$ respectively).

3.3. Microtensile bond strength (μTBS) testing and nanoleakage

The number premature failures are shown in Table 3. The cross-product interaction was statistically significant for microtensile bond strength ($p = 0.003$) and nanoleakage ($p = 0.002$) tests. A significant

Table 1
Means and standard deviations of bacterial inhibition halo sizes (mm) observed by the different copper-containing adhesives against *S. mutans* in the immediate time.*

	Copper (%)						
	0 (control)	0.0075	0.015	0.060	0.1	0.5	1
Inhibition halo sizes (mm)	4.87 A	7.59 B	8.25 B	9.12 B	10.92C	11.51C	11.87C
Standard deviation	0.41	0.98	0.94	0.65	0.93	0.79	0.52

* Means identified with the same letter are statistically similar. (Tukeýs test, $p \geq 0.05$).

Table 2
Means and standard deviations of the immediate and 2-year Knoop microhardness (KNH) and degree of conversion (%) obtained in each experimental condition.*

Adhesive	Immediate KNH	2-year KHN	*in vitro* DC	*in situ* DC
0% (control)	5.47 ± 0.49 A	5.77 ± 0.12 A,B	95.97 ± 0.26 a	96.17 ± 1.79 A
0.0075%	5.73 ± 0.22 A,B	10.4 ± 1.2 F	94.95 ± 0.88 a	96.87 ± 0.45 A
0.015%	5.77 ± 0.24 A,B	8.58 ± 1.2 E,F	93.27 ± 0.08 a	95.33 ± 0.50 A
0.060%	6.77 ± 0.14C,D	10.3 ± 1.4 F	94.31 ± 0.49 a	95.36 ± 1.55 A
0.1%	7.03 ± 0.12 D,E	14.3 ± 1.6 G	92.53 ± 1.21 a	94.82 ± 1.12 A
0.5%	7.53 ± 0.17 E	16.9 ± 2.0 F,G	92.56 ± 0.68 a	93.50 ± 2.56 A
1%	6.33 ± 0.10 B,C	12.7 ± 2.8 F	72.64 ± 3.06 b	85.63 ± 3.42 B

* Comparisons are valid only within test. Means identified with the same capital, lowercase or superscript letters are statistically similar (Tukeýs test, $p \geq 0.05$).

Table 3
Number (%) of specimens according to fracture mode for all experimental groups.*

Adhesive	Immediate				2-years			
	A/M	CD	CR	PF	A/M	CD	CR	PF
0% (control)	35 (100)	0 (0)	0 (0)	0 (0)	35 (100)	0 (0)	0 (0)	0 (0)
0.0075%	34 (97)	0 (0)	1 (3)	0 (0)	31 (89)	3 (8)	0 (0)	1 (3)
0.015%	33 (94)	0 (0)	2 (6)	0 (0)	31 (89)	0 (0)	1 (3)	3 (8)
0.060%	31 (89)	0 (0)	4 (11)	0 (0)	33 (94)	1 (3)	1 (3)	0 (0)
0.1%	29 (83)	4 (11)	2 (6)	0 (0)	33 (94)	2 (6)	0 (0)	0 (0)
0.5%	29 (83)	1 (3)	5 (14)	0 (0)	33 (94)	1 (3)	1 (3)	0 (0)
1%	31 (89)	1 (3)	3 (8)	0 (0)	31 (89)	1 (3)	3 (8)	0 (0)

* A/M = adhesive/mixed fracture mode; CD = cohesive in dentine; CR = cohesive in resin or; PF = premature failures.

decrease in the μTBS after 2 years of water storage were observed for the control group, as well as, for copper-containing adhesives with concentrations up to 0.015 wt% (Table 4; $p = 0.003$). However, this decrease was much more pronounced for the control group (reduction of 43%) compared with the adhesives containing 0.0075 and 0.0015% of copper (reduction of 22 to 25%). Regarding to nanoleakage, a significant increase in the nanoleakage after 2 years was only detected for the control group (Table 4; $p = 0.002$). The other copper-containing adhesives showed similar percentage of nanoleakage between the immediate and 2-year periods (Fig. 3).

3.4. Identification of copper within adhesive specimens and in the adhesive/hybrid layers by EDX

Representative EDX spectrum of the adhesive specimens with 0.060% copper (Fig. 4) shows the presence of copper in the surface and underneath the adhesive. The same pattern was observed for all copper-containing adhesive (data not shown). Representative EDX spectrums of the hybrid layer produced with adhesives containing 0.015%, 0.060% and 0.5% (Fig. 5) show the presence of copper either in the immediate and 2-year periods. In control adhesive specimens, as expected, copper was not observed in the hybrid layer in any time. In the immediate period and 2-year periods, all copper-containing adhesives present copper in the hybrid layer of specimens bonded with adhesives containing copper concentration equal to or higher than 0.06% (Fig. 5).

4. Discussion

In this study, the incorporation of copper nanoparticles in the formulation of a simplified ER adhesive showed a significant antimicrobial activity against *S. mutans* regardless of the concentration. This is in agreement with other studies that evaluated lower [41] and higher copper concentrations [40] than the ones investigated in this study.

It was already demonstrated that the antibacterial activity of copper nanoparticles is dependent on its size and concentration [52,53]. We observed that the inhibition halo against *S. mutans* was higher with increased copper nanoparticles concentration. Nevertheless, the mechanism by which copper nanoparticles exert their antibacterial effect remains obscure. Previous studies mentioned that the antibacterial effect of the copper nanoparticles might be due to interactions with −SH groups of key microbial enzymes, leading to their denaturation [54,55].

Additionally, copper can bind to amine and carboxylic groups on the surface of the microorganism modifying their cell membranes [56,57].

Additionally, after entering the cell, copper nanoparticles may disrupt biochemical processes [58,59] and can bind to DNA molecules. This changes the DNA helical structure by crosslinking within and between nucleic acid strands and alters the DNA replication of the microorganisms [55,60]. A more recent theory is called “Trojan horse effect”, where the acidic lysosomal environment (pH 5.5) is capable of promoting nanoparticles degradation/corrosion, which converts core metals to ions and therefore toxic substances. The intercellular release of free ions generates a high volume of reactive oxygen species in mitochondria or can induce the malfunction of other organelles [61]. As one can see there are numerous hypothesis to explain the antimicrobial mechanisms of copper nanoparticles, but it is not fully understood yet and should be matter of further studies.

The idea behind the incorporation of copper into adhesive formulations was to keep its antimicrobial properties for longer periods of times. An earlier study [62] measured the copper release of disc-like

Table 4
Means and the respective standard deviations of microtensile bond strength (μTBS, MPa) and nanoleakage (NL, %), obtained in each experimental condition.*

Adhesive	μTBS		NL	
	Immediate	2-Year	Immediate	2-Year
0% (control)	37.3 ± 2.5C	21.2 ± 2.5 E	16.3 ± 3.0 a	30.4 ± 4.2 d
0.0075%	38.2 ± 2.2C	29.5 ± 1.0 D	12.1 ± 2.6 a,b,c	12.9 ± 4.7 a,b
0.015%	42.4 ± 3.0 B,C	31.8 ± 2.6 D	9.2 ± 3.1 b,c	12.1 ± 4.6 a,b
0.060%	41.7 ± 2.2 B,C	34.7 ± 3.2C,D	11.4 ± 2.5 a,b,c	14.6 ± 2.3 a,b
0.1%	40.8 ± 2.0 B,C	34.2 ± 3.1C,D	9.3 ± 2.3 b,c	9.1 ± 2.5 b,c
0.5%	48.2 ± 4.1 A,B	43.3 ± 1.3 B,C,	5.2 ± 3.1 c	8.9 ± 3.1 b,c
1%	36.3 ± 3.3C	42.3 ± 3.2 B,C	4.3 ± 2.4 c	8.3 ± 3.2 b,c

* Comparisons are valid only within test. Means identified with the same capital or lowercase letters are statistically similar (Tukeýs test, $p \geq 0.05$).

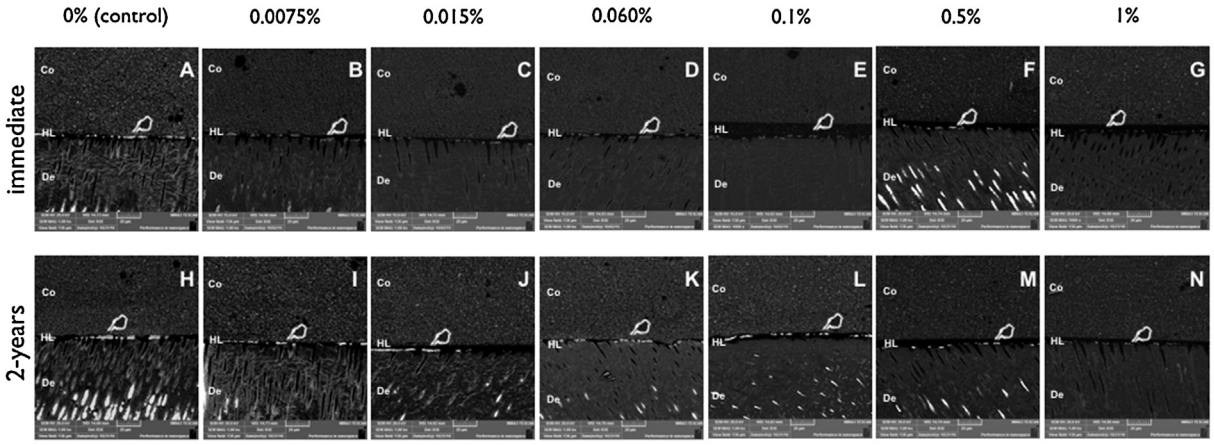

Fig. 3. Representative back-scattering SEM images of the resin–dentine interfaces bonded with the ER adhesive in the immediate time (A–G) or after 2-year of water storage (H–N) according to the different experimental conditions. Only few and superficial areas of NL were observed within HL (white pointer in A–G) in the immediate time. However, a significant increase in the NL was observed, mainly in the control group after 2-year of water storage. It was possible to observe that, for all groups of copper-containing adhesive (I–N), after 2-year, the NL is lower when compared to the control group (H) (Co = composite; HL = hybrid layer and De = dentine).

adhesive specimens and showed that the mechanism behind the copper release in the first 28 days was governed by Fickian diffusion and biexponential equation. According to this equation, the time interval to attain a 50% release of the copper content is longer than one year [62]. In this study, we observed that the presence of copper after 2-year in bonded adhesive interfaces is dependent on the copper concentration. Copper was only found in adhesives interfaces that contained concentrations of copper equal to or higher than 0.06%, which is a promising finding. Considering that copper concentration equal to or higher than 0.06% was capable to produce higher inhibition halo against *S.mutans* higher than the control adhesive, one may speculate that this slow release over time may supplement antimicrobial activity of the adhesive apart from the expected sealing and retention. This however, should be seen as a hypothesis since the mechanism and amount of copper release from disc specimens are rather different that of thin layers bonded to the dentin substrate. Although the presence of copper was observed after two years by EDX in adhesive interfaces bonded with copper in concentrations equal to or higher than 0.06% we do not know whether this interface is capable to exert the same antimicrobial activity than disc-like specimens of adhesives. Indeed, even the disc-like specimens after 2 years did not show any antimicrobial activity probably due to the high and fast release of copper in the aqueous environment [62].

Microhardness test is usually used as an indirect measurement of the degree of conversion of polymeric materials [63]. The increased microhardness values observed with adhesives containing copper concentrations equal to or higher than 0.06% can be explained by the increased fraction of filler particles by addition of copper nanoparticles. There is a positive correlation between the volume fraction of filler and the Knoop hardness of composites [64] since filler particles are harder than the organic phase of the material.

Except from the adhesive with the highest copper concentration (1%), no significant reductions of the degree of conversion were observed in the experimental groups compared to control under the *in vitro* and *in situ* degree of conversion methodologies. This means that the addition of copper in concentrations up to 0.5% does not interfere with the well-balanced monomer/solvent blend, which may be due to the good chemical compatibility when added to adhesive systems [40,41]. On the other hand, at 1% concentration, copper may act as a plasticizer within the polymer network. We observed in this group (1% copper) that the adhesive underwent a plasticization process within the bottle, and this preliminary plasticization process within the bottle may have reduced the degree of conversion by preventing monomers from getting closer one another during the initiation and polymerization process and might explain the lower degree of conversion values. More interesting were the microhardness values observed after 2 years of water storage. The significant higher microhardness at 2 years is probably the result of greater degrees of polymerization and dark reaction, forming tough, glassy, low stress homogeneous glassy cross-linked networks [65], less prone to the plasticization of water in the long term as it will be explained in more details in this discussion.

Regarding the durability of the resin-dentin interfaces, we observed a reduction of approximately 43% in the resin-dentin bond strength values and an increase of 86% in nanoleakage values in copper-free control adhesives. The degradation of these adhesive interfaces from the control group can be explained by the collagenolytic and gelatinolytic activity on the partially demineralized dentin after application of simplified ER adhesives by activation of metalloproteinases (MMPs) [66–68] and cysteine-cathepsins (CTs) [69–71]. This results in a self-degradation of partially infiltrated collagen fibrils [72] and yields reductions of bond strength values over time [15].

On the other hand this was not observed in the copper-containing adhesives with concentrations ranging from 0.006 to 1%. However, even for copper-containing adhesives ranging of 0.0075 and 0.0015%, the degradation was much less pronounced (reduction of 22–25% of μTBS and increasing of 5–30% in nanoleakage) than for the control group (reduction of 43% of μTBS and increasing of 86% in NL). This indicates that, copper-containing adhesives produced interfaces capable of minimizing degradation of the resin-dentin bonded interfaces dentin after 2-year of water storage, when compared with copper-free adhesives.

The good resistance of copper-containing adhesives on the long-term properties can be explained because of several factors. It has been showed that copper can increase the strength of the collagen network, one of the component of the hybrid layer, because the collagen crosslinking enzyme, lysyl oxidase (LOX), is copper dependent [73,74], and thus copper has an indirect effect as a cross-linking agent. This cross-linker action of copper may increase the resistance of collagen, fact that indirectly increases the bond strength. By increasing the collagen strength and the adhesive itself, this substrate becomes less susceptible to the effects of proteolytic enzymes such as MMPs and CTs. Sabatini et al. [40] showed that, copper has the ability to inhibit the dentin MMP-2 [75], and the secretion of tissue inhibitors of MMPs (TIMPs) [76], causing lower degradation pattern in the resin/dentine interface.

The present study was capable to demonstrate that the addition of copper nanoparticles to adhesives provided them with immediate antimicrobial properties and although these characteristics were not maintaining after 2-year of water storage, their presence in the adhesive/hybrid layer was enough to preserve the resin-dentin interface from degradation and reduction of bond strength values.

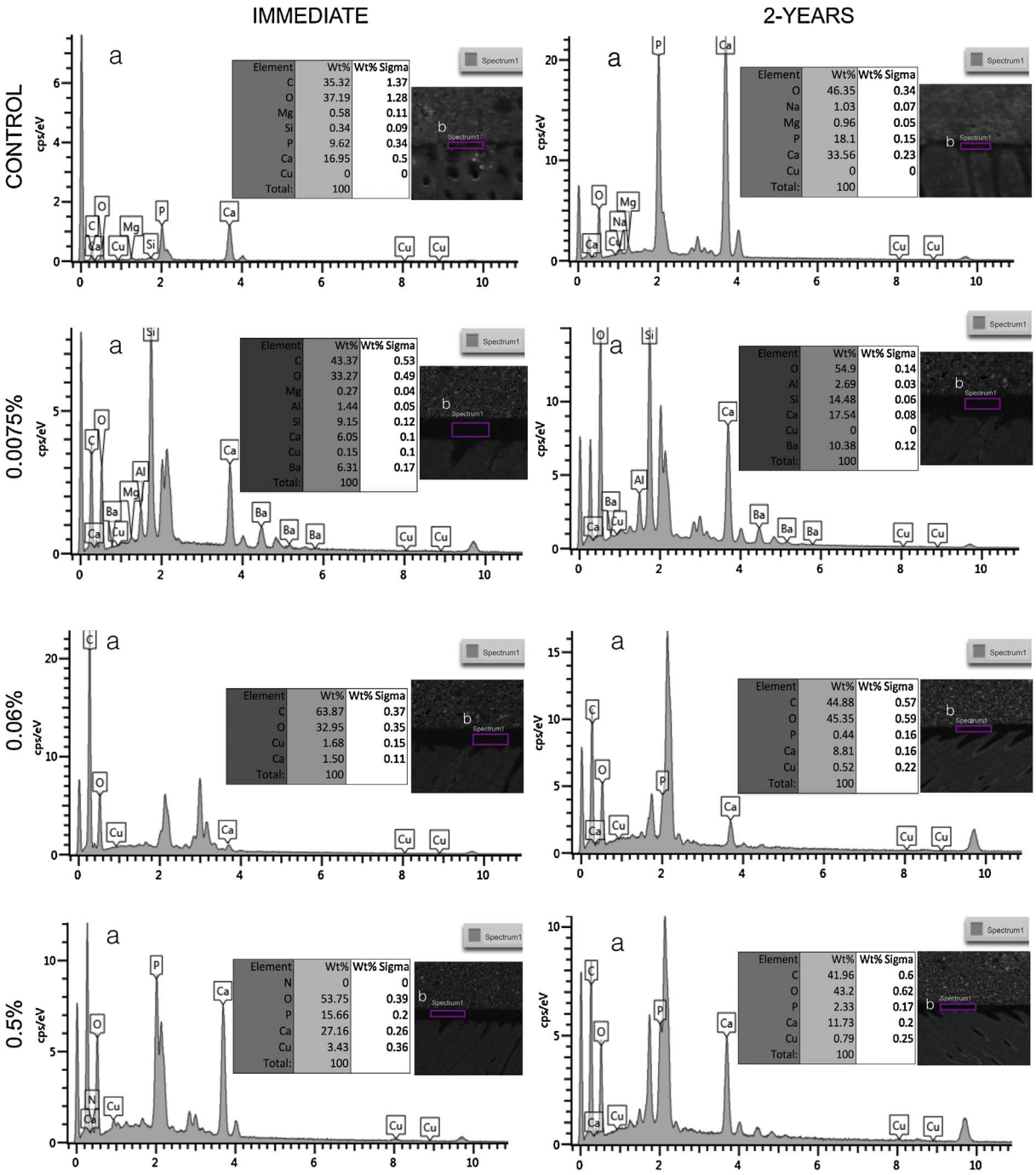

Fig. 4. EDX spectrum of the resin–dentine interfaces bonded with the ER adhesive in the immediate time or after 2-year of water storage for control, 0.015%, 0.060% and 0.5% copper-containing adhesive. EDX spectra (a) from selected area of the hybrid layer outlined by a magenta rectangle in (b). The figure table summarizes the elemental composition of the sample area outlined.

Additionally, copper addition was responsible for an increase in the mechanical properties of the adhesives after long-term water storage. However, further studies are still required to evaluate if copper-containing adhesive interfaces are less prone to degradation under oral conditions and in more challenging conditions such as cariogenic and erosive environments.

5. Conclusion

The addition of copper nanoparticles in concentrations up to 0.5% in the two-step etch-and-rinse adhesive system is a feasible approach and may be an alternative to adhesive interfaces with immediate antimicrobial properties, increased immediate and 2-year bond strength of resin-dentine interfaces, and also the mechanical properties of the adhesive formulations after 2-year of water storage.

Acknowledgements

This study was partially supported by the Conselho Nacional de Desenvolvimento Científico e Tecnológico (CNPq) under grants 304104/2013-9 and 305588/2014-1.

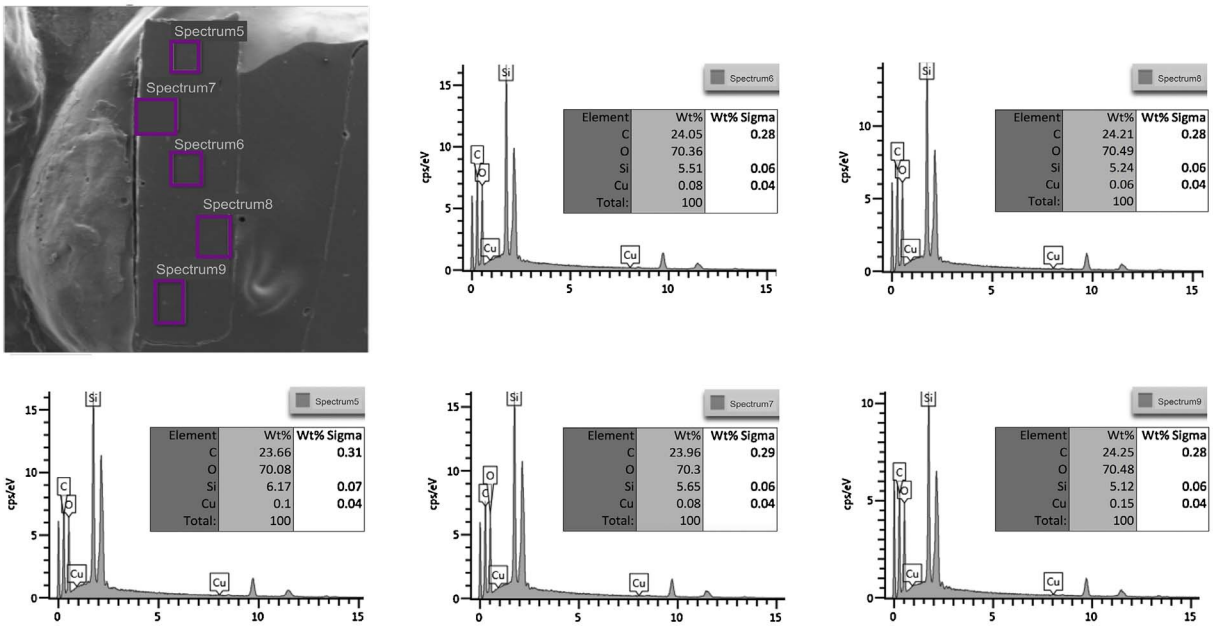

Fig. 5. EDX spectrum of the body of the ER adhesive in the immediate time 0.060% copper-containing adhesive. EDX spectra (a-d) from different selected area of the adhesive body outlined by a magenta rectangle in (b). The figure table summarizes the elemental composition of the sample area outlined.

References

[1] V. Deligeorgi, I. Mjör, N. Wilson, An overview of reasons for the placement and replacement of restorations, Prim. Dent. Care 8 (2001) 5–11.
[2] I.A. Mjor, J.E. Moorhead, J.E. Dahl, Reasons for replacement of restorations in permanent teeth in general dental practice, Int. Dent. J. 50 (2000) 361–366.
[3] M.S. Cenci, L.M. Tenuta, T. Pereira-Cenci, A.A. Del Bel Cury, J.M. ten Cate, J.A. Cury, Effect of microleakage and fluoride on enamel-dentine demineralization around restorations, Caries Res. 42 (2008) 369–379.
[4] J.L. Ferracane, Resin composite–state of the art, Dent. Mater. 27 (2011) 29–38.
[5] J.L. Ferracane, Resin-based composite performance: are there some things we can't predict? Dent. Mater. 29 (2013) 51–58.
[6] V.V. Gordan, J.L. Riley 3rd, S. Geraldeli, D.B. Rindal, V. Qvist, J.L. Fellows, H.P. Kellum, G.H. Gilbert, Repair or replacement of defective restorations by dentists in The Dental Practice-Based Research Network, J. Am. Dent. Assoc. 143 (2012) 593–601.
[7] N.J. Opdam, E.M. Bronkhorst, J.M. Roeters, B.A. Loomans, A retrospective clinical study on longevity of posterior composite and amalgam restorations, Dent. Mater. 23 (2007) 2–8.
[8] N. Beyth, A.J. Domb, E.I. Weiss, An in vitro quantitative antibacterial analysis of amalgam and composite resins, J. Dent. 35 (2007) 201–206.
[9] F. Li, M.D. Weir, J. Chen, H.H. Xu, Effect of charge density of bonding agent containing a new quaternary ammonium methacrylate on antibacterial and bonding properties, Dent. Mater. 30 (2014) 433–441.
[10] R.P. Barbosa, T. Pereira-Cenci, W.M. Silva, F.H. Coelho-de-Souza, F.F. Demarco, M.S. Cenci, Effect of cariogenic biofilm challenge on the surface hardness of direct restorative materials in situ, J. Dent. 40 (2012) 359–363.
[11] M.M. Zalkind, O. Keisar, P. Ever-Hadani, R. Grinberg, M.N. Sela, Accumulation of Streptococcus mutans on light-cured composites and amalgam: an in vitro study, J. Esthet. Dent. 10 (1998) 187–190.
[12] T.M. Auschill, N.B. Arweiler, M. Brecx, E. Reich, A. Sculean, L. Netuschil, The effect of dental restorative materials on dental biofilm, Eur. J. Oral Sci. 110 (2002) 48–53.
[13] H.J. Busscher, M. Rinastiti, W. Siswomihardjo, H.C. van der Mei, Biofilm formation on dental restorative and implant materials, J. Dent. Res. 89 (2010) 657–665.
[14] I. Nedeljkovic, W. Teughels, J. De Munck, B. Van Meerbeek, K.L. Van Landuyt, Is secondary caries with composites a material-based problem? Dent. Mater. 31 (2015) 247–277.
[15] L. Breschi, A. Mazzoni, A. Ruggeri, M. Cadenaro, R. Di Lenarda, E. De Stefano Dorigo, Dental adhesion review: aging and stability of the bonded interface, Dent. Mater. 24 (2008) 90–101.
[16] P. Spencer, Q. Ye, J. Park, E.M. Topp, A. Misra, O. Marangos, Y. Wang, B.S. Bohaty, V. Singh, F. Sene, J. Eslick, K. Camarda, J.L. Katz, Adhesive/Dentin interface: the weak link in the composite restoration, Ann. Biomed. Eng. 38 (2010) 1989–2003.
[17] P. Totiam, C. Gonzalez-Cabezas, M.R. Fontana, D.T. Zero, A new in vitro model to study the relationship of gap size and secondary caries, Caries Res. 41 (2007) 467–473.
[18] M.A. Borges, I.C. Matos, L.C. Mendes, A.S. Gomes, M.S. Miranda, Degradation of polymeric restorative materials subjected to a high caries challenge, Dent. Mater. 27 (2011) 244–252.
[19] M. Bourbia, D. Ma, D.G. Cvitkovitch, J.P. Santerre, Y. Finer, Cariogenic bacteria degrade dental resin composites and adhesives, J. Dent. Res. 92 (2013) 989–994.
[20] J.G. Thomas, L.A. Nakaishi, Managing the complexity of a dynamic biofilm, J. Am. Dent. Assoc. 137 (Suppl) (2006) 10s–15s.
[21] L. Chen, H. Shen, B.I. Suh, Antibacterial dental restorative materials: a state-of-the-art review, Am. J. Dent. 25 (2012) 337–346.
[22] A.R. Cocco, W.L. Rosa, A.F. Silva, R.G. Lund, E. Piva, A systematic review about antibacterial monomers used in dental adhesive systems: current status and further prospects, Dent. Mater. 31 (2015) 1345–1362.
[23] S. Imazato, S. Ma, J.H. Chen, H.H. Xu, Therapeutic polymers for dental adhesives: loading resins with bio-active components, Dent. Mater. 30 (2014) 97–104.
[24] J.R. Morones, J.L. Elechiguerra, A. Camacho, K. Holt, J.B. Kouri, J.T. Ramirez, M.J. Yacaman, The bactericidal effect of silver nanoparticles, Nanotechnology 16 (2005) 2346–2353.
[25] A.K. Chatterjee, R.K. Sarkar, A.P. Chattopadhyay, P. Aich, R. Chakraborty, T. Basu, A. simple robust method for synthesis of metallic copper nanoparticles of high antibacterial potency against E. coli, Nanotechnology 23 (2012) 085103.
[26] A.M. Essa, M.K. Khallaf, Antimicrobial potential of consolidation polymers loaded with biological copper nanoparticles, BMC Microbiol. 16 (2016) 144.
[27] O.V. Zakharova, A.Y. Godymchuk, A.A. Gusev, S.I. Gulchenko, I.A. Vasyukova, D.V. Kuznetsov, Considerable variation of antibacterial activity of Cu nanoparticles suspensions depending on the storage time, dispersive medium, and particle sizes, BioMed Res. Int. 2015 (2015) 412530.
[28] N.R. Chowdhury, M. MacGregor-Ramiasa, P. Zilm, P. Majewski, K. Vasilev, 'Chocolate' silver nanoparticles: synthesis, antibacterial activity and cytotoxicity, J. Colloid Interface Sci. 482 (2016) 151–158.
[29] M. Skladanowski, P. Golinska, K. Rudnicka, H. Dahm, M. Rai, Evaluation of cytotoxicity, immune compatibility and antibacterial activity of biogenic silver nanoparticles, Med. Microbiol. Immunol. 205 (2016) 603–613.
[30] K.Y. Yoon, J. Hoon Byeon, J.H. Park, J. Hwang, Susceptibility constants of Escherichia coli and Bacillus subtilis to silver and copper nanoparticles, Sci. Total Environ. 373 (2007) 572–575.
[31] J.P. Ruparelia, A.K. Chatterjee, S.P. Duttagupta, S. Mukherji, Strain specificity in antimicrobial activity of silver and copper nanoparticles, Acta Biomater. 4 (2008) 707–716.
[32] A.P. Ingle, N. Duran, M. Rai, Bioactivity, mechanism of action, and cytotoxicity of copper-based nanoparticles: a review, Appl. Microbiol. Biotechnol. 98 (2014) 1001–1009.
[33] M.S. Usman, N.A. Ibrahim, K. Shameli, N. Zainuddin, W.M. Yunus, Copper nanoparticles mediated by chitosan: synthesis and characterization via chemical methods, Molecules 17 (2012) 14928–14936.
[34] M.S. Usman, M.E. El Zowalaty, K. Shameli, N. Zainuddin, M. Salama, N.A. Ibrahim, Synthesis, characterization, and antimicrobial properties of copper nanoparticles, Int. J. Nanomed. 8 (2013) 4467–4479.
[35] M.G. Schmidt, H.H. Attaway Iii, S.E. Fairey, L.L. Steed, H.T. Michels, C.D. Salgado, Copper continuously limits the concentration of bacteria resident on bed rails within the intensive care unit, Infect. Control Hosp. Epidemiol. 34 (2013) 530–533.
[36] Y. Wang, X.Y. Zi, J. Su, H.X. Zhang, X.R. Zhang, H.Y. Zhu, J.X. Li, M. Yin, F. Yang, Y.P. Hu, Cuprous oxide nanoparticles selectively induce apoptosis of tumor cells, Int. J. Nanomed. 7 (2012) 2641–2652.
[37] K. Zhang, M.A. Melo, L. Cheng, M.D. Weir, Y. Bai, H.H. Xu, Effect of quaternary ammonium and silver nanoparticle-containing adhesives on dentin bond strength and dental plaque microcosm biofilms, Dent. Mater. 28 (2012) 842–852.
[38] M.A. Melo, L. Cheng, K. Zhang, M.D. Weir, L.K. Rodrigues, H.H. Xu, Novel dental

adhesives containing nanoparticles of silver and amorphous calcium phosphate, Dent. Mater. 29 (2013) 199–210.
[39] W.G. Renne, A. Lindner, A.S. Mennito, K.A. Agee, D.H. Pashley, D. Willett, D. Sentelle, M. Defee, M. Schmidt, C. Sabatini, Antibacterial properties of copper iodide-doped glass ionomer-based materials and effect of copper iodide nanoparticles on collagen degradation, Clin. Oral Investig. 21 (2017) 369–379.
[40] C. Sabatini, A.S. Mennito, B.J. Wolf, D.H. Pashley, W.G. Renne, Incorporation of bactericidal poly-acrylic acid modified copper iodide particles into adhesive resins, J. Dent. 43 (2015) 546–555.
[41] L. Argueta-Figueroa, R.J. Scougall-Vilchis, R.A. Morales-Luckie, O.F. Olea-Mejia, An evaluation of the antibacterial properties and shear bond strength of copper nanoparticles as a nanofiller in orthodontic adhesive, Aust. Orthod. J. 31 (2015) 42–48.
[42] M. Gosau, M. Haupt, S. Thude, M. Strowitzki, B. Schminke, R. Buergers, Antimicrobial effect and biocompatibility of novel metallic nanocrystalline implant coatings, J. Biomed. Mater. Res. B Appl. Biomater. 104 (2016) 1571–1579.
[43] J. Rosenbaum, D.L. Versace, S. Abbad-Andallousi, R. Pires, C. Azevedo, P. Cenedese, P. Dubot, Antibacterial properties of nanostructured Cu-TiO2 surfaces for dental implants, Biomater. Sci. 5 (2017) 455–462.
[44] K.S. Gregson, H. Shih, R.L. Gregory, The impact of three strains of oral bacteria on the surface and mechanical properties of a dental resin material, Clin. Oral Investig. 16 (2012) 1095–1103.
[45] R. Huang, M. Li, R.L. Gregory, Effect of nicotine on growth and metabolism of Streptococcus mutans, Eur. J. Oral Sci. 120 (2012) 319–325.
[46] G.C. Martins, M.M. Meier, A.D. Loguercio, A. Reis, J.C. Gomes, O.M. Gomes, Effects of adding barium-borosilicate glass to a simplified etch-and-rinse adhesive on radiopacity and selected properties, J. Adhes. Dent. 16 (2014) 107–114.
[47] V. Hass, M. Dobrovolski, C. Zander-Grande, G.C. Martins, L.A. Gordillo, L. Rodrigues Accorinte Mde, O.M. Gomes, A.D. Loguercio, A. Reis, Correlation between degree of conversion, resin-dentin bond strength and nanoleakage of simplified etch-and-rinse adhesives, Dent. Mater. 29 (2013) 921–928.
[48] V. Hass, I. Luque-Martinez, N.B. Sabino, A.D. Loguercio, A. Reis, Prolonged exposure times of one-step self-etch adhesives on adhesive properties and durability of dentine bonds, J. Dent. 40 (2012) 1090–1102.
[49] A. Reis, R.H. Grande, G.M. Oliveira, G.C. Lopes, A.D. Loguercio, A 2-year evaluation of moisture on microtensile bond strength and nanoleakage, Dent. Mater. 23 (2007) 862–870.
[50] C.A. Schneider, W.S. Rasband, K.W. Eliceiri, NIH Image to ImageJ: 25 years of image analysis, Nat. Methods 9 (2012) 671–675.
[51] J. Perdigão, M.A. Munoz, A. Sezinando, I.V. Luque-Martinez, R. Staichak, A. Reis, A.D. Loguercio, Immediate adhesive properties to dentin and enamel of a universal adhesive associated with a hydrophobic resin coat, Oper. Dent. 39 (2014) 489–499.
[52] A. Azam, A.S. Ahmed, M. Oves, M.S. Khan, A. Memic, Size-dependent antimicrobial properties of CuO nanoparticles against Gram-positive and −negative bacterial strains, Int. J. Nanomed. 7 (2012) 3527–3535.
[53] T. Pandiyarajan, R. Udayabhaskar, S. Vignesh, R.A. James, B. Karthikeyan, Synthesis and concentration dependent antibacterial activities of CuO nanoflakes, Mater. Sci. Eng. C Mater. Biol. Appl. 33 (2013) 2020–2024.
[54] A.M. Schrand, M.F. Rahman, S.M. Hussain, J.J. Schlager, D.A. Smith, A.F. Syed, Metal-based nanoparticles and their toxicity assessment, Wiley Interdiscip. Rev. Nanomed. Nanobiotechnol. 2 (2010) 544–568.
[55] R.P. Allaker, K. Memarzadeh, Nanoparticles and the control of oral infections, Int. J. Antimicrob. Agents 43 (2014) 95–104.
[56] K. Blecher, A. Nasir, A. Friedman, The growing role of nanotechnology in combating infectious disease, Virulence 2 (2011) 395–401.
[57] G. Ren, D. Hu, E.W. Cheng, M.A. Vargas-Reus, P. Reip, R.P. Allaker, Characterisation of copper oxide nanoparticles for antimicrobial applications, Int. J. Antimicrob. Agents 33 (2009) 587–590.
[58] J.H. Kim, H. Cho, S.E. Ryu, M.U. Choi, Effects of metal ions on the activity of protein tyrosine phosphatase VHR: highly potent and reversible oxidative inactivation by Cu2+ ion, Arch. Biochem. Biophys. 382 (2000) 72–80.
[59] J.S. Kim, E. Kuk, K.N. Yu, J.H. Kim, S.J. Park, H.J. Lee, S.H. Kim, Y.K. Park, Y.H. Park, C.Y. Hwang, Y.K. Kim, Y.S. Lee, D.H. Jeong, M.H. Cho, Antimicrobial effects of silver nanoparticles, Nanomedicine 3 (2007) 95–101.
[60] R.P. Allaker, The use of nanoparticles to control oral biofilm formation, J. Dent. Res. 89 (2010) 1175–1186.
[61] S. Sabella, R.P. Carney, V. Brunetti, M.A. Malvindi, N. Al-Juffali, G. Vecchio, S.M. Janes, O.M. Bakr, R. Cingolani, F. Stellacci, P.P. Pompa, A general mechanism for intracellular toxicity of metal-containing nanoparticles, Nanoscale 6 (2014) 7052–7061.
[62] M.F. Gutierrez, P. Malaquias, T.P. Matos, A. Szesz, S. Souza, J. Bermudez, A. Reis, A.D. Loguercio, P.V. Farago, Mechanical and microbiological properties and drug release modeling of an etch-and-rinse adhesive containing copper nanoparticles, Dent. Mater. 33 (2017) 309–320.
[63] J.P. DeWald, J.L. Ferracane, A comparison of four modes of evaluating depth of cure of light-activated composites, J. Dent. Res. 66 (1987) 727–730.
[64] K.H. Chung, E.H. Greener, Correlation between degree of conversion, filler concentration and mechanical properties of posterior composite resins, J. Oral Rehabil. 17 (1990) 487–494.
[65] H.B. Song, N. Sowan, P.K. Shah, A. Baranek, A. Flores, J.W. Stansbury, C.N. Bowman, Reduced shrinkage stress via photo-initiated copper(I)-catalyzed cycloaddition polymerizations of azide-alkyne resins, Dent. Mater. 32 (2016) 1332–1342.
[66] A. Mazzoni, F.D. Nascimento, M. Carrilho, I. Tersariol, V. Papa, L. Tjaderhane, R. Di Lenarda, F.R. Tay, D.H. Pashley, L. Breschi, MMP activity in the hybrid layer detected with in situ zymography, J. Dent. Res. 91 (2012) 467–472.
[67] A. Mazzoni, D.H. Pashley, Y. Nishitani, L. Breschi, F. Mannello, L. Tjaderhane, M. Toledano, E.L. Pashley, F.R. Tay, Reactivation of inactivated endogenous proteolytic activities in phosphoric acid-etched dentine by etch-and-rinse adhesives, Biomaterials 27 (2006) 4470–4476.
[68] Y. Nishitani, M. Yoshiyama, B. Wadgaonkar, L. Breschi, F. Mannello, A. Mazzoni, Activation of gelatinolytic/collagenolytic activity in dentin by self-etching adhesives, Eur. J. Oral Sci. 114 (2006) 160–166.
[69] I.L. Tersariol, S. Geraldeli, C.L. Minciotti, F.D. Nascimento, V. Paakkonen, M.T. Martins, M.R. Carrilho, D.H. Pashley, F.R. Tay, T. Salo, L. Tjaderhane, Cysteine cathepsins in human dentin-pulp complex, J. Endod. 36 (2010) 475–481.
[70] F.D. Nascimento, C.L. Minciotti, S. Geraldeli, M.R. Carrilho, D.H. Pashley, F.R. Tay, H.B. Nader, T. Salo, L. Tjaderhane, I.L. Tersariol, Cysteine cathepsins in human carious dentin, J. Dent. Res. 90 (2011) 506–511.
[71] C.M. Vidal, L. Tjaderhane, P.M. Scaffa, I.L. Tersariol, D. Pashley, H.B. Nader, F.D. Nascimento, M.R. Carrilho, Abundance of MMPs and cysteine cathepsins in caries-affected dentin, J. Dent. Res. 93 (2014) 269–274.
[72] D.H. Pashley, F.R. Tay, C. Yiu, M. Hashimoto, L. Breschi, R.M. Carvalho, S. Ito, Collagen degradation by host-derived enzymes during aging, J. Dent. Res. 83 (2004) 216–221.
[73] B. Marelli, D. Le Nihouannen, S.A. Hacking, S. Tran, J. Li, M. Murshed, C.J. Doillon, C.E. Ghezzi, Y.L. Zhang, S.N. Nazhat, J.E. Barralet, Newly identified interfibrillar collagen crosslinking suppresses cell proliferation and remodelling, Biomaterials 54 (2015) 126–135.
[74] R.B. Rucker, T. Kosonen, M.S. Clegg, A.E. Mitchell, B.R. Rucker, J.Y. Uriu-Hare, C.L. Keen, Copper, lysyl oxidase, and extracellular matrix protein cross-linking, Am. J. Clin. Nutr. 67 (1998) 996s–1002.
[75] A.P. de Souza, R.F. Gerlach, S.R. Line, Inhibition of human gingival gelatinases (MMP-2 and MMP-9) by metal salts, Dent. Mater. 16 (2000) 103–108.
[76] A. Simeon, H. Emonard, W. Hornebeck, F.X. Maquart, The tripeptide-copper complex glycyl-L-histidyl-L-lysine-Cu2+ stimulates matrix metalloproteinase-2 expression by fibroblast cultures, Life Sci. 67 (2000) 2257–2265.